DESIGN AND EXPERIMENTAL STUDY OF AN INTELLIGENT INSPECTION UGV FOR AGRICULTURAL APPLICATIONS
/
农业智能检测无人小车的设计与试验研究

Shiyu ZHANG*[1)], Meiqin WANG[1)], Xiaozhen LI[1)], Yitong GOU[1)]
[1)] School of Intelligent Manufacturing, Nanyang Institute of Technology, Nanyang, Henan, 473004, China
Tel: +86 18716310821; E-mail: 3011118@nyist.edu.cn
Corresponding author: Shiyu Zhang
DOI: https://doi.org/10.35633/inmateh-78-43

Keywords: *Agricultural intelligence, Obstacle-Avoidance UGV, STM32, Multi-sensor*

ABSTRACT
Agricultural intelligence is an important trend in the development of modern agriculture. However, agricultural UGVs that rely on manual intervention or fixed path planning suffer from low operational efficiency and poor adaptability. To address these issues, an obstacle-avoidance UGV based on an STM32 microcontroller is designed in this study. The UGV uses a motor driver chip for motion control, Bluetooth for signal transmission, and an integrated image transmission module, which effectively improves obstacle recognition and rapid obstacle avoidance compared with conventional agricultural UGVs. Experimental results show that the steering angle control accuracy of the vehicle ranges from 90.0% to 98.9%, while the obstacle detection accuracy ranges from 92.5% to 98.3%. The UGV is able to stably complete obstacle-avoidance tasks under field conditions.

摘要
农业机械化向智能化转型已成为现代农业发展的重要趋势，传统农用小车在存在依赖人工干预或固定路径规划的作业模式效率低、适应性差等问题。针对这一问题，本论文设计一款基于 STM32 微控制器的田间避障小车，该小车利用电机驱动芯片进行驱动、蓝牙进行信号传输，并搭载图像传输模块进行图像的实时传输，有效解决传统农用小车在障碍物识别、快速避障方面的问题。试验表明，小车转向角度控制准确率 90.0%~98.9%，障碍物测距精确度 92.5%~98.3%，该小车在田间环境中可稳定完成田间避障任务。

INTRODUCTION
Rapid population growth and the shortage of arable land resources are major challenges facing global agriculture. According to UN projections, by 2050, the global population is expected to reach 10 billion, with food demand projected to increase by over 60% (*Huang et al., 2025*). Recently, the problem of population aging has gradually become the focus of social attention, especially in rural areas. It is urgent to improve agricultural production efficiency. The above problems can be solved by unmanned agricultural machinery equipped with high-precision navigation (*Li et al., 2016; Wang et al., 2020*). However, such machinery relies on expensive sensors (LiDAR and GPS) and high-computing power platforms, which imposes high costs and excessively high technical barriers on smallholder farmers when purchasing intelligent agricultural machinery (*Qi et al., 2019; Jiang et al., 2022*). Currently, there is a lack of solutions that combine low cost, high adaptability and easy promotion. Relying on the obstacle avoidance system composed of embedded hardware, the embedded technology with low cost and high reliability provides a new solution for smallholder farmers (*Lan et al., 2022*).

In the 60s of the 20th century, researchers began to explore the evolution of modern agriculture, and the concept of precision agriculture was initially formed in the 80s. At this stage, agricultural mechanization gradually began to be popularized, and mechanical facilities such as tractors began to gradually replace human and animal power (*Thanpattranon et al., 2016*). In the early 90s of the 20th century, researchers successively carried out research on agricultural precision, the purpose of which was to use computer technology to change the traditional production mode, and integrate modern technologies such as GPS and geographic information system into the development of traditional agriculture to achieve the goal of precision agricultural operations (*Luciano et al., 2019*). At this stage, when agricultural machinery encounters complex road conditions, stability cannot be guaranteed and human intervention is required. At the same time, due to limited computing power and hardware costs, the system still cannot meet commercial standards (*Bac et al., 2016*).

Shiyu Zhang, Lecturer Ph.D. Eng.; Wang Meiqin, B. Stud. Eng.; Xiaozhen Li, Lecturer M.S. Eng; Yitong Gou, B.Stud.Eng.

At the beginning of the 21st century, the scientific and technological level of countries around the world has risen significantly, multi-sensor technology and machine vision technology have also developed rapidly, and smart agricultural machinery has entered a stage of vigorous development. *Arad et al.* (*2020*) showed a fully autonomous tractor equipped with a 360° camera and radar at the Autonomous Concept Vehicle launch event. In the CROPS robot project in Europe (*Nissimovs et al., 2015*), researchers have developed an obstacle avoidance robot specifically for orchards, which relies on stereoscopic vision to achieve the purpose of avoiding fruit trees in the orchard. The "AgriRobo" developed by Japanese researchers uses infrared and ultrasonic sensors to achieve obstacle avoidance for small fields.

In the past decade, researchers from various countries have applied deep learning to the field of image recognition, such as the John Deere X9 harvester, which combines an AI obstacle avoidance system with a high probability of successful obstacle avoidance (*Xu et al., 2022; Zhao et al., 2022*). The Oz robot used radar and camera sensors to avoid obstacles (*Nakao et al., 2017*). Currently, researchers from various countries are conducting research on the popularization of unmanned technology, they have collaborated on obstacle avoidance technology and the Internet of Things to build an "unmanned" ecosystem (*Huang et al., 2020*).

In the field of smart agriculture, however, hardware and algorithms have been greatly improved, there are few field obstacle avoidance smart agricultural machinery for small farmers, and the price of commercial products is still expensive, which is not conducive to promotion and popularization (*Qin et al., 2018; Han et al., 2020; Nazarahari et al., 2019*). In this paper, STM32 is selected as the controller of the UGV, the DC motor is driven by the control chip of the motor, and the camera is used to collect image information, and the collected image information is transmitted to the mobile phone for display through WIFI, so as to achieve obstacle avoidance in the farmland environment.

MATERIALS AND METHODS

General design

The functions of the agricultural intelligent UGV designed in this paper are as follows: (1) Motion function: mainly including the essential motion functions such as forward, backward, left and right turn and speed change of the UGV; (2) Obstacle avoidance function: it can effectively avoid the obstacles encountered, so as to achieve barrier-free driving; (3) Wireless communication function: connected through WIFI wireless signal, real-time remote control and video information display of the UGV. The system of the field obstacle avoidance is divided into two aspects: hardware and software, and the overall framework is shown in Fig.1.

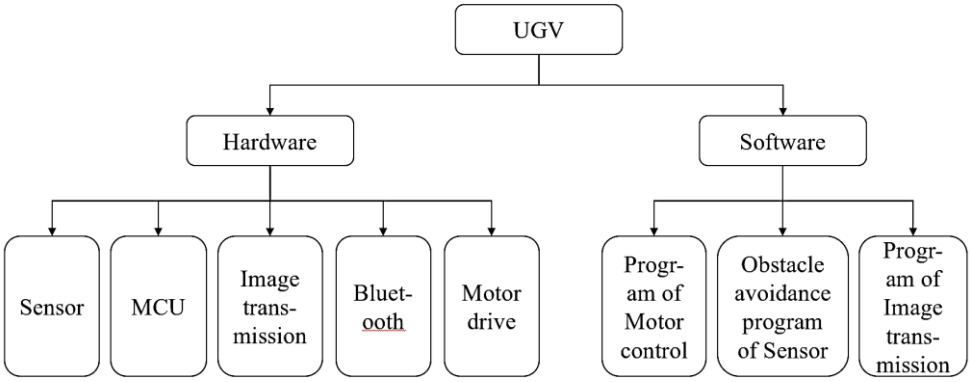

Fig. 1 - The overall framework of UGA

Hardware

The hardware of the field obstacle avoidance UGV is designed for the two key functions of obstacle ranging and avoidance. The hardware is composed of MCU, a Bluetooth, a motor drive, an image transmission module, an ultrasonic and a power supply.

The main controller is the key component of the system, and in order to meet the reliability requirements of complex scenarios in the field, STM32F103C8T6 is selected as the 32-bit microcontroller for this paper. The Bluetooth module provides signal transmission for the UGV, and JDY-31 is the best candidate for this paper based on many considerations. In order to reduce the risk of mud jamming and improve the wading ability, the DC motor model selected in this paper is TT motor. The power module is to smoothly convert the 7V-12V voltage output of the battery pack into 5V or 3.3V required by each unit, so that the main controller, Bluetooth module and image transmission module work normally at the safe voltage, and the power module model selected in this paper is MP1584EN.

The image transmission module transmits the image/video data captured by the camera from the UGV to the receiver in real time, and the image transmission module selected in this paper is ESP32-CAM. The ultrasonic module detects the distance of the obstacle in front in real time, and assists the UGV to make obstacle avoidance decisions through this distance data, the ultrasonic module model of this paper is HC-SR04.s

The process of obstacle avoidance

Obstacle avoidance means that during the automatic driving of the UGV (*Demin et al., 2019; Dai et al., 2019; Labbe et al., 2019*), when the ultrasonic sensor detects that there is an obstacle in front and the distance is less than the set value, the UGV stops and turns, so that the UGV avoids the obstacle. The flow chart of obstacle avoidance is shown in Figure 2.

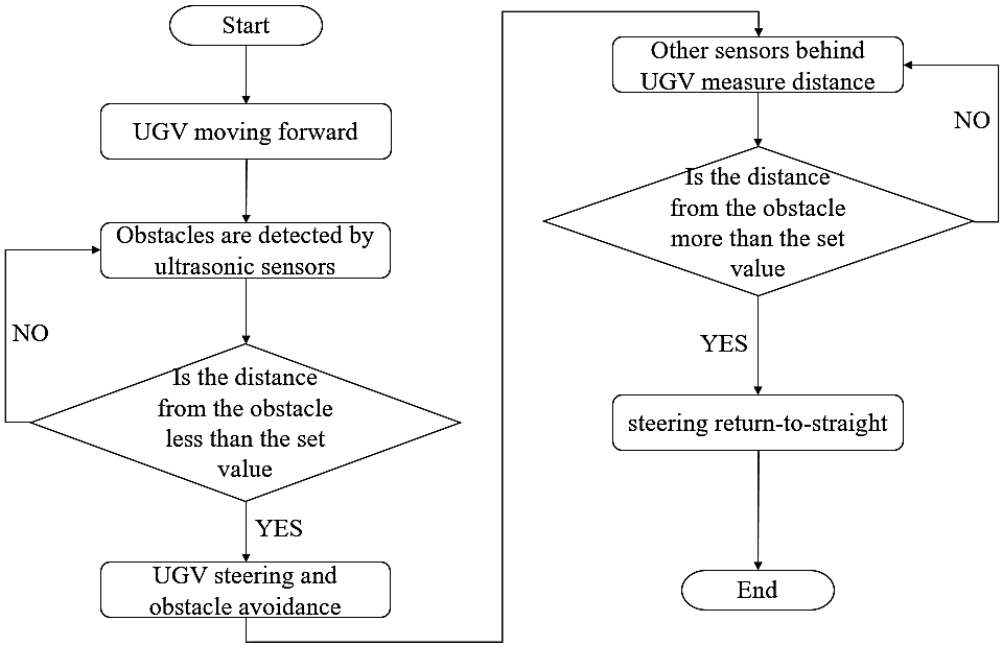

Fig. 2 - The flow chart of obstacle avoidance

Motor control

In this system, the UGV uses two DC motors to achieve motion control. To accurately control the motion state of the UGV, a motor drive scheme based on PWM (Pulse Width Modulation) speed regulation and GPIO (General Purpose Input/Output) direction control is designed. The motor control flowchart is shown in Figure 3, and the motor control truth table is presented in Table 1.

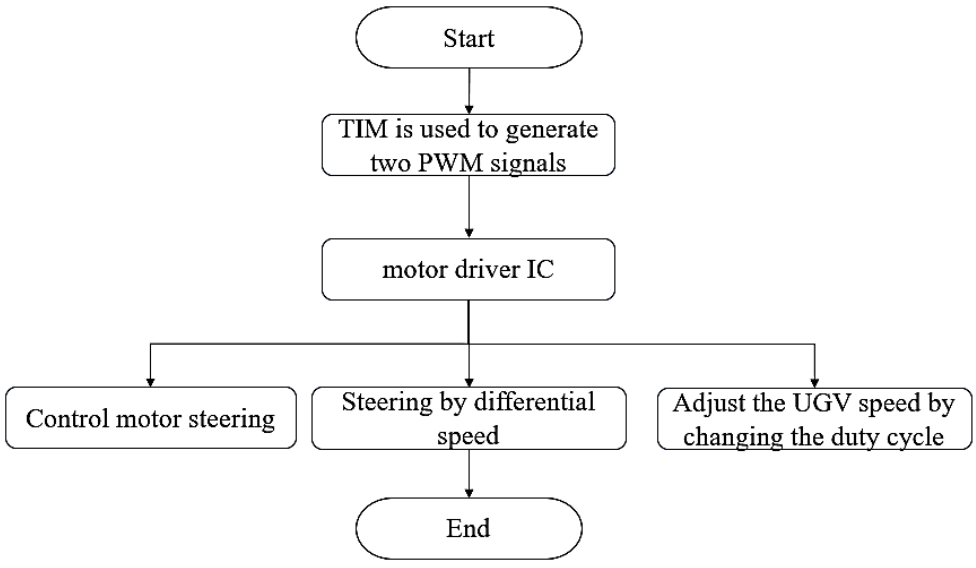

Fig. 3 - Motor control flowchart

Table 1

Motor control truth table

Motor operation	PWM duty cycle
Forward rotation	> 0
Reverse rotation	< 0
Stop	= 0

The obstacle avoidance process

The ultrasonic obstacle avoidance process is based on the use of ultrasonic waves to measure the distance to obstacles. The distance calculation formula is given in Eq. (1):

$$D = \frac{CountNum \times 0.034}{2} \quad (1)$$

where D is the ranging distance, cm; $CountNum$ is the echo high-level duration recorded by the timer, μs; 0.034 is the speed of sound in air, corresponding to 340 m/s=0.034 cm/μs**.**

The distance between the UGV and the obstacle is first measured. If the measured distance is greater than the preset threshold, the UGV continues to move forward. If the distance is less than the threshold, the UGV stops and, under microcontroller control, drives a servo to detect the available space in the left and right directions. The UGV then moves in the direction with greater available space. The steering angle of the UGV is controlled by a dedicated function that linearly maps an angle range of 0°~180° to a pulse width range of 500 μs~2500 μs. The corresponding relationship is expressed as follows:

$$PulseWidth = \frac{Angle}{180} \times 2000 + 500 \quad (2)$$

where: $Pulse\ Width$ is the calculated high-level pulse width; $Angle$ is the target rotation angle of the servo.

The whole obstacle avoidance process: First, distance information is obtained from three ultrasonic sensors positioned at the front, left rear, and right rear of the UGV. When the distance to an obstacle in the front direction is detected to be less than 25 cm, the UGV stops immediately. The microcontroller then determines the avoidance direction based on the distance information from the side sensors. If the distance on the right side is greater than 50 cm, the servo is reset to 90°, and the UGV turns right for 1 s to bypass the obstacle. If the right side does not satisfy this condition but the left-side distance is greater than 50 cm, the UGV turns left for 1 s to perform obstacle avoidance. After detouring, when the rear ultrasonic sensor detects that the distance to the obstacle is greater than 30 cm, the UGV turns back to the original driving direction. If neither side provides sufficient clearance, a conservative strategy is adopted, and the UGV reverses for 1 s. Finally, after completing steering or reversing, the servo is reset to the forward position (90°). If no obstacle is detected within the preset threshold in the front direction, the UGV continues straight ahead.

The AUV prototype

The interface designed in this study is used to monitor the road conditions in front of the UGV in real time through an image transmission module. The interface was developed using the MIT App Inventor platform. After configuration, the interface was packaged as an APK installation file. Once installed on a mobile phone, the surrounding environment in front of the UGV can be monitored in real time.

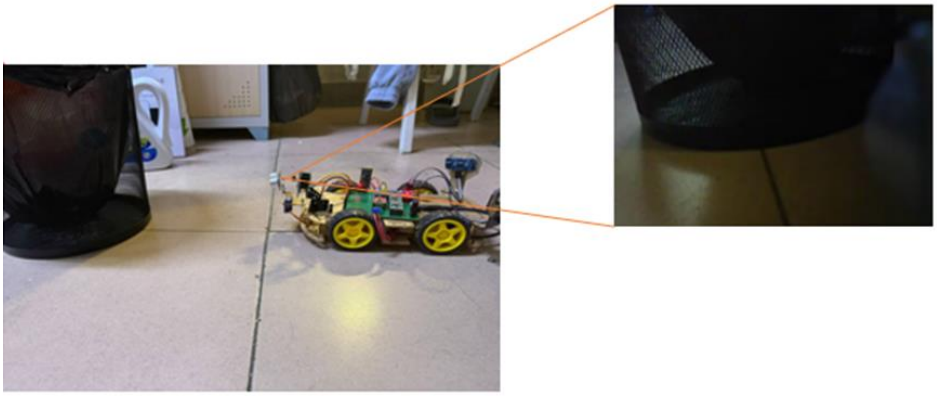

Fig. 4 -The AUV prototype

RESULTS

After the UGV is assembled and debugged, the three functions of the UGV such as motor drive, obstacle ranging, and UGV obstacle avoidance need to be tested.

Motor drive test

Motor drive is the most fundamental function of the system developed in this study. In this experiment, the steering angle of the UGV is a key factor affecting obstacle avoidance performance. First, the UGV was driven along a straight path. When an obstacle was encountered, the UGV turned to the right by 90°. The steering angle after turning was then measured. The procedure for measuring the steering angle is illustrated in Fig. 5. The UGV moving along a straight path is shown in Fig. 5a, and the measured steering angle after turning is shown in Fig. 5b.

(a) straight driving (b) angle measurement after steering

Fig. 5 - Measurement process of the steering angle

First, the optimal combination of motor differential speed and steering angle was tested under indoor conditions. In this experiment, a right turn with a steering duration of 1000 ms was taken as an example, and the corresponding combinations of motor differential speed and steering angle are listed in Table 2. As shown in Table 2, when the duty cycle of one motor was set to 40% and the duty cycle of the other motor was set to 0%, with a steering time of 1000 ms, the resulting steering angle of the UGV was closest to the target angle of 90°, achieving an accuracy of 97.8%. Therefore, in the subsequent experiments, the steering control parameters were selected as a 40% duty cycle for one motor, a 0% duty cycle for the other motor, and a steering time of 1000 ms.

Table 2

Combinations of motor differential duty cycles and steering angle

Duty cycle of left motor	Duty cycle of right motor	Turning time / ms	Set angle/°	Actual angle/°	Relative accuracy
50	0	1000	90	115	72.2%
40	0	1000	90	88	97.8%
30	0	1000	90	69	76.7%

Secondly, steering accuracy was further verified through experiments conducted on rough outdoor pavement and field pavement. The test results under different environments are presented in Table 3.

Table 3

Steering angle test results under different road conditions

Parameter	Ordinary road	Field road
Set angle / °	90	90
Actual angle / °	89	85
Relative accuracy	98.9%	94.4%

As shown in Table 3, when the steering angle was set to 90°, the steering accuracy of the UGV was 98.9% on the ordinary road and 94.4% on the field road surface. The lower accuracy observed under field conditions is mainly due to the complex and uneven terrain, where tire slippage on muddy surfaces may occur, resulting in reduced steering accuracy.

To further evaluate the steering accuracy of the UGV under field conditions, steering tests were conducted at target angles of 80°, 60°, 40°, and 20°, and the corresponding accuracies were calculated to assess whether the performance met expectations. The results of the field steering tests are presented in Table 4. As shown in the table, when operating on the field road surface, the steering accuracy of the UGV was approximately 94%. Therefore, the steering control parameters selected in this study were a duty cycle of 40% for one motor, a duty cycle of 0% for the other motor, and a steering time of 1000 ms.

Table 4

Field steering test results

Set angle / °	Relative accuracy
80	94.4%
60	95.2%
40	93.9%
20	95.3%

Obstacle distance measurement

Obstacle distance measurement is a key component of this study. Ultrasonic ranging experiments were conducted under multiple scenarios to verify the adaptability of the UGV to complex field environments. Scene 1 represents a field environment with dense weeds, Scene 2 represents a rough field road environment, and Scene 3 represents a wet field environment after rainfall. The ranging results under different scenarios are shown in Figs. 6-8, and the corresponding measurement data are presented in Table 5.

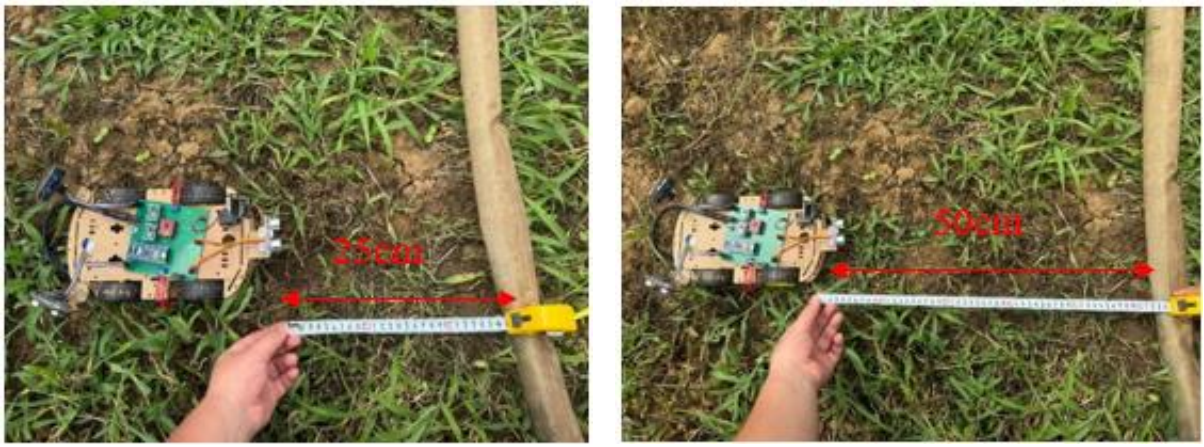

(a) 25 cm from the obstacle (b) 50 cm from the obstacle

Fig. 6 - Ultrasonic ranging results in Scene 1

(a) 25 cm from the obstacle (b) 50 cm from the obstacle

Fig. 7 - Ultrasonic ranging results in Scene 2

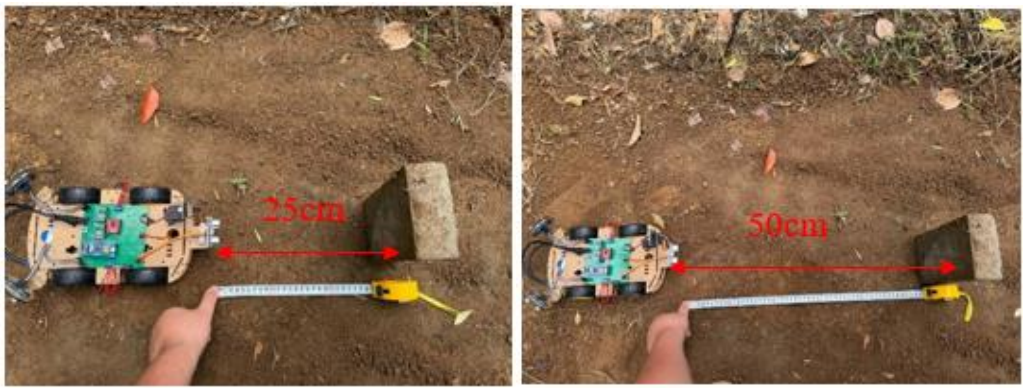

(a) 25 cm from the obstacle (b) 50 cm from the obstacle

Fig. 8 - Ultrasonic ranging results in Scene 3

Table 5

Ultrasonic ranging test results under different scenarios

	Scene 1	Scene 2	Scene 3	Absolute average error	Relative accuracy
25cm	26.9cm	26.8cm	26.9cm	1.9cm	92.5%
50cm	52.7cm	51.4cm	53.8cm	2.6cm	94.7%

From the ranging results shown in Figs. 6-8 and Table 5, it can be observed that when the obstacle distance was 25 cm, the average measurement error across the three scenarios was 1.9 cm, corresponding to a relative accuracy of 92.5%. When the obstacle distance was 50 cm, the average error was 2.6 cm, with a relative accuracy of 94.7%. These results indicate that under different environmental conditions and detection distances, the relative ranging accuracy of the proposed method remains between 92.5% and 94.7%, which meets the application requirements.

Field obstacle avoidance test

After completing the above experiments, a field obstacle avoidance test was conducted. The obstacle avoidance process of the UGV is illustrated in Fig. 9.

Figure 9a shows the UGV moving forward when the distance to the obstacle becomes less than 25 cm. Figure 9b shows that the UGV stops immediately when the ultrasonic sensor detects an obstacle at a distance of 25 cm. Figures 9c and 9d show the ultrasonic detection of the available space on the right and left sides of the UGV, respectively. Figure 9e shows that the UGV selects the direction with greater available space and turns to the right. Figure 9f shows that the rear ultrasonic sensor detects a distance greater than 30 cm between the UGV and the obstacle. Figure 9g shows the UGV turning left to bypass the obstacle, and Figure 9h shows that after bypassing the obstacle, the UGV returns to its original driving direction. The experimental results demonstrate that the UGV can autonomously complete obstacle avoidance maneuvers on field roads.

(a) UGV moving forward *(b) Obstacle detected by the UGV* *(c) UGV detecting the available space on the right side*

(d) UGV detecting the available space on the left side

(e) UGV turning right

(f) Ultrasonic detection indicating that the distance from the obstacle was greater than 30 cm

(g) UGV moving straight after turning left;

(h) UGV bypassing the obstacle

Fig. 9 - Obstacle avoidance process of the UGV

CONCLUSIONS

To address the obstacle avoidance challenges faced by traditional agricultural vehicles in complex field environments, a low-cost obstacle avoidance system based on an STM32 microcontroller was designed and implemented in this study. Through theoretical analysis, hardware development, and field test validation, the following main conclusions were obtained:

(1) Low-cost hardware integration scheme. A modular design approach was adopted to integrate low-cost components, including the HC-SR04 ultrasonic sensor, TB6612 motor driver, JDY-31 Bluetooth communication module, and ESP32-CAM image transmission module. The overall hardware cost of the system is lower than that of comparable solutions, providing a high cost–performance ratio and meeting the economic and reliability requirements of smallholder farmers.

(2) Embedded control system development. A real-time control architecture was developed based on the STM32F103C8T6 microcontroller, and closed-loop control of dual DC motors was achieved using PWM pulse width modulation. Experimental results show that the steering angle control accuracy of the system under complex field terrain conditions ranges from 90.0% to 98.9%.

(3) Multi-sensor obstacle avoidance mechanism. Real-time field images are acquired by a camera module and transmitted to a computer for monitoring, while obstacle distances are detected using ultrasonic sensors. Field tests indicate that the relative ranging accuracy of the obstacle detection system ranges from 92.5% to 98.3%, enabling reliable obstacle avoidance in agricultural field environments.

However, the proposed agricultural UGV still exhibits limitations when operating in highly complex farmland terrain. Future work should focus on enhancing environmental perception through multi-sensor data fusion and artificial intelligence techniques. This would enable more advanced intelligent decision-making functions, such as real-time crop growth monitoring, automated pest and disease identification, and precision pesticide application, thereby supporting more comprehensive and automated management in intelligent agricultural systems.

ACKNOWLEDGEMENT

Funding: This work was supported by the "Science and Technology research Project of Nanyang (24KJGG048)"; the "Doctoral Research Foundation Project of Nanyang Institute of Technology (grant numbers NGBJ-2025-07)"; and the "Interdisciplinary Science Research Project of Nanyang Institute of Technology (24NGJY006)".

REFERENCES

[1] Arad B., Balendonck J., Barth R., Ohad B. Yael E., Thomas H. (2020). Development of a sweet pepper harvesting robot. *Journal of Field Robotics*, Vol.37, No.6, pp. 1027-1039. Beer-Sheva/ Israel.

[2] Bac W., Tim R, Roi R., Sigal B., Jochen H., Eldert J. (2016). Analysis of a motion planning problem for sweet-pepper harvesting in a dense obstacle environment. *Biosystems Engineering*, Vol.146, pp.85-97. Wageningen/ The Netherlands.

[3] Dai J.C., Yan L., Liu H., Chen C., Huo L. (2019). An offline coarse-to-fine precision optimization algorithm for 3D laser SLAM point cloud (3D 激光 SLAM 点云的离线粗到精精度优化算法). *Remote Sensing*, Vol.11, No.20, 2352. Hubei/China.

[4] Demin F., Boucheloukh A., Nemera A. (2019). An adaptive SVSF-SLAM algorithm in dynamic environment for cooperative unmanned vehicles. *IFAC Papers OnLine*, Vol.52, No.15, pp.394-399. Algiers/Algeria.

[5] Deng X., Li R. F., Zhao L.J.,Wang K., Gui X. (2021). Multi-obstacle path planning and optimization for mobile robot (移动机器人多障碍路径规划与优化). *Expert Systems with Applications*, Vol.183, No.30, pp.115445. Heilongjiang/China.

[6] Eil F.H., Ibraheem I.K., Azar A.T. (2020). Grid -based mobile robot path planning using aging-based ant colony optimization algorithm in static and dynamic environments. *Sensors*, Vol.20, No.7, pp. 25-32. Giza/Egypt.

[7] Han Y. Q., Wei C., Li R., Wang J., Yu H. (2020). A novel cooperative localization method based on IMU and UWB (基于 IMU 和 UWB 的新型协作定位方法). *Sensors*, Vol.20, No.2, pp.467. Beijing/China.

[8] Jiang S., Zhang M., Li X. (2022). Development of navigation and control technology for autonomous mobile equipment in greenhouse (设施内自主移动装备导航控制技术研究进展). *Journal of Chinese Agricultural Mechanization*, Vol.43, No.3, pp.159-169. Jiangsu/China.

[9] Labbe M., Michaud F. (2019). RTAB-Map as an open source LiDAR and visual simultaneous localization and mapping library for large-scale and long-term online operation. *Journal of Field Robotics*, Vol.36, No.2, pp.416-446. Sherbrooke/Canada.

[10] Lan Y., Yan Y., Wang B., Song C., Wang G. (2022). Current status and future development of the key technologies for intelligent pesticide spraying robots (智能施药机器人关键技术研究现状及发展趋势). *Transactions of the Chinese Society of Agricultural Engineering*, Vol.38, No.20, pp.30-40. Shandong/China.

[11] Lao C., Li P., Feng Y. (2021). Path planning of greenhouse robot based on fusion of improved A* algorithm and dynamic window approach (基于改进 A*与 DWA 算法融合的温室机器人路径规划). *Transactions of the Chinese Society for Agricultural Machinery*, Vol.52, No.1, pp.14-22. Beijing/China.

[12] Luciano C., Filippo B., Domenico L. (2019). A small versatile electrical robot for autonomous spraying in agriculture. *AgriEngineering,* Vol.1, No.3, pp.391-402. Catania/Italy.

[13] Nakao N., Suzuki H., Kitajima T. (2017). Path planning and traveling control for pesticide-spraying robot in greenhouse. *Journal of Signal Processing*, Vol.21, No.4, pp. 175-178. Tokushima/Japan.

[14] Nazarahari M., Khanmirza E., Doostie S. (2019). Multi-objective multi-robot path planning in continuous environment using an enhanced genetic algorithm. *Expert Systems with Applications*, Vol.115, pp.106-120. Edmonton/Canada.

[15] Nissimov S., Goldberger J., Alchanatis V. (2015). Obstacle detection in a greenhouse environment using the Kinect sensor. *Computers and Electronics in Agriculture*, Vol.113, pp. 104-115. Tel Aviv-Yafo/ Israel.

[16] Qi F., Li K., Li S., He F., & Zhou X. (2019). Development of intelligent equipment for protected horticulture in world and enlightenment to China (世界设施园艺智能化装备发展对中国的启示研究). *Transactions of the Chinese Society of Agricultural Engineering*, Vol.35, No.2, pp.183-195. Beijing/China.

[17] Qin T., Li P., Shen S. J. (2018). VINS-Mono: A robust and versatile monocular visual-inertial state estimator (一种稳健且多功能的单眼视觉惯性状态估计器). *IEEE Transactions on Robotics*, Vol.34, No.4, pp.1004-1020. Hong Kong/China.

[18] Song B. Y., Wang Z. D., Zou L. (2021). An improved PSO algorithm for smooth path planning of mobile robots using continuous high-degree Bezier curve. *Applied Soft Computing*, Vol.100, pp.106960. Shandong/China.

[19] Thanpattranon P., Ahamed T., Takigawa T. (2016). Navigation of autonomous tractor for orchards and plantations using a laser range finder: automatic control of trailer position with tractor. *Biosystems Engineering*, Vol. 147, pp.90-103. Tsukuba/Japan.

[20] Li H. J., Zhang J.S. (2020). Robust visual line-following navigation system for humanoid robots (人形机器人的稳健视觉线条跟踪导航系统). *Artificial Intelligence Review*, Vol.53, No.1, pp. 653-670. Fujian/China.

[21] Wang F. T., Fan C. C., Li Z. D. (2020). Application status and development trend of robots in the field of facility agriculture (机器人在设施农业领域应用现状及发展趋势分析). *Journal of Chinese Agricultural Mechanization*, Vol.41, No.3, pp. 93-98, 120. Anhui/China.

[22] Xu T. Y., Feng S., Chen C. (2018). Research on design method of self-tracking spray vehicle in solar greenhouse (日光温室自主寻迹喷药车设计方法研究). *Journal of Shenyang Agricultural University*, Vol.49, No.4, pp.440-446. Liaoning/China.

[23] Zhang X. Y., Zou Y.S. (2021). Collision-free path planning for automated guided vehicles based on improved A* algorithm. *Systems Engineering-Theory & Practice*, Vol. 41, No.1, pp. 240-246. Shanghai/China.

[24] Zhao Z. X., Zhang Y.C., Long L., Lu Z., & Shi J. (2022). Efficient and adaptive LiDAR-visual-inertial odometry for agricultural unmanned ground vehicle. *International Journal of Advanced Robotic Systems*, Vol. 19, No.2, pp. 1-15. Beijing/China.

[25] Zhao Z. X., Zhang Y.C., Shi J.L. (2022). Robust LiDAR-inertial odometry with ground condition perception and optimization algorithm for UGV. *Sensors*, Vol. 22, No.19, pp.7424. Beijing/China.